Laminin 332 Is Indispensable for Homeostatic Epidermal Differentiation Programs

JID Open

Check for updates

Raneem Tayem[1], Catherin Niemann[1,2], Monika Pesch[1], Jessica Morgner[3,4], Carien M. Niessen[2,5,6], Sara A. Wickström[3,6,7,8] and Monique Aumailley[1]

The skin epidermis is attached to the underlying dermis by a laminin 332 (Lm332)—rich basement membrane. Consequently, loss of Lm332 leads to the severe blistering disorder epidermolysis bullosa junctionalis in humans and animals. Owing to the indispensable role of Lm332 in keratinocyte adhesion in vivo, the severity of the disease has limited research into other functions of the protein. We have conditionally disrupted Lm332 expression in basal keratinocytes of adult mice. Although blisters develop along the interfollicular epidermis, hair follicle basal cells provide sufficient anchorage of the epidermis to the dermis, making inducible deletion of the *Lama3* gene compatible with life. Loss of Lm332 promoted the thickening of the epidermis and exaggerated desquamation. Global RNA expression analysis revealed major changes in the expression of keratins, cornified envelope proteins, and cellular stress markers. These modifications of the keratinocyte genetic program are accompanied by changes in cell shape and disorganization of the actin cytoskeleton. These data indicate that loss of Lm332-mediated progenitor cell adhesion alters cell fate and disturbs epidermal homeostasis.

INTRODUCTION

Laminin 332 (Lm332) is the central component in a multi-protein network that constitutes the basement membrane attaching the skin epidermis to the dermis. Laminins are glycoproteins endowed with structural, adhesive, signaling, and mechanical functions through which they control the homeostasis of cells and tissues (Aumailley, 2013). Alterations in laminin expression or processing and mutations in laminin-coding genes are associated with pathologies such as cancer, autoimmune diseases, or inborn disorders (Durbeej, 2015; Funk et al., 2018; Qin et al., 2017; Simon and Bromberg, 2017). In particular, mutations in the genes coding for any one of the α3, β3, and γ2 chains of Lm332 lead to

absence or strong reduction of the protein, causing the severe skin-blistering disorder epidermolysis bullosa junctionalis (Aumailley et al., 2006; Kiritsi et al., 2013; Uitto et al., 1994). The condition is often associated with early death, thus restricting studies on the role of Lm332 in vivo.

Using an inducible conditional transgenic mouse model in which the disruption of the *Lama3* gene in the basal keratinocytes (KCs) of adult mice results in a progressive loss of Lm332, we unequivocally showed that Lm332 is crucial to maintain the physical attachment of the epidermis to the dermis (Pesch et al., 2017). These transgenic mice develop blisters at the interfollicular epidermis (IFE) and epidermal thickening, but the epidermis remains anchored to the dermis within the hair follicles (Pesch et al., 2017). Thus, the model is compatible with life in contrast to the lethality associated with the constitutive deletion of Lm332, allowing us to study the longer-term consequences of the loss of Lm332 in vivo. It is particularly well-suited for determining which cellular activities shown to be under the control of Lm332 in vitro are also under its control in adult skin in vivo. Except for the essential role of Lm332 for stable adhesion of KCs, firmly established by clinical, genetics, and biological studies of junctional epidermolysis bullosa, in vivo studies supporting the role of Lm332 for the control of other cellular activities are very scarce and are limited to newborns or mouse embryos.

To uncover how the loss of Lm332 leads to morphological changes in the epidermis, especially the thickening, we performed RNA sequencing (RNA-seq) of the epidermal cells from transgenic and control mice. Of the 1,961 genes that were significantly regulated in the epidermis of Lm332-depleted mice, genes coding for keratins, cornified envelope proteins, and cell stress markers were strongly

[1]Center for Biochemistry, Faculty of Medicine, University of Cologne, Cologne, Germany; [2]Center for Molecular Medicine Cologne, University of Cologne, Cologne, Germany; [3]Paul Gerson Unna Group 'Skin Homeostasis and Ageing', Max Planck Institute for Biology of Ageing, Cologne, Germany; [4]Division of Molecular Pathology, Oncode Institute, Netherlands Cancer Institute, Amsterdam, The Netherlands; [5]Medical Faculty, Department of Cell Biology of the Skin, University of Cologne, Cologne, Germany; [6]Cologne Excellence Cluster on Cellular Stress Responses in Aging-Associated Diseases (CECAD), University of Cologne, Cologne, Germany; [7]Helsinki Institute of Life Science, University of Helsinki, Helsinki, Finland; and [8]Wihuri Research Institute, Biomedicum Helsinki, University of Helsinki, Helsinki, Finland

Correspondence: Monique Aumailley, Center for Biochemistry, Faculty of Medicine, University of Cologne, Cologne, Germany. E-mail: aumailley@uni-koeln.de

Abbreviations: IFE, interfollicular epidermis; K, keratin; KC, keratinocyte; Lama3 KO, Lama3e knockout; Lama3 KO/B+, Lama3e knockout mouse with blister; Lm332, laminin 332; QRT-PCR, quantitative real-time reverse transcriptase—PCR; RNA-seq, RNA sequencing

upregulated. In addition, there were profound changes in the cell shape and disorganization of the actin cytoskeleton, pointing to substantial perturbation of epidermal homeostasis in the absence of Lm332.

RESULTS

Blistering and epidermal thickening during an inducible loss of *Lama3*

The loss of *Lama3* and consequently of Lm332 in the adult epidermis was induced by putting *Lama3*flox/flox/K14-CreERT (*Lama3*e knockout [*Lama3*e KO]) mice on a chow diet containing tamoxifen for 8–12 weeks. Whereas the Lm332 in the skin of *Lama3e KO* mice is reduced to 5–30% that of the controls, blisters develop along the IFE (Pesch et al., 2017) (Supplementary Figure S1). H&E staining of back skin sections revealed epidermal thickening above the blisters of *Lama3*e KO mice when compared with that of the controls (Figure 1a). Thickening increased proportionally with the extent of blistering. When blistering affected at least 30% of the length of the dermal–epidermal junction, epidermal thickness above the blisters was two- to six-fold that of adjacent areas devoid of blisters or that of littermate controls (Figure 1b) (mice 11–21, referred to as *Lama3*e KO mice with blister [*Lama3*e KO/B⁺] in the remaining part of this paper), whereas when blistering affected <30% of the dermal–epidermal junction length in *Lama3*e KO mice, the epidermal thickness was similar to that of the controls (Figure 1b) (mice 1–10, referred to as *Lama3*e KO mice without blister). Interestingly, epidermal thickness correlated to blistering but not to Lm332 levels in the skin (Supplementary Figure S1), suggesting that thickening is not a direct consequence of the decreased concentration of Lm332.

We further observed an expansion of the cornified layer above the blisters of *Lama3*e KO/B⁺ mice (Figure 1a). These results indicate that the absence of epidermal anchorage to the dermis through Lm332 leads to an abnormally thick epidermis.

Upregulation of genes coding for cornified envelop proteins and FLG during the loss of Lm332

To assess how Lm332 regulates epidermal homeostasis, freshly isolated KCs from the skin of control and *Lama3*e KO/B⁺ mice in which at least 30% of the IFE shows blisters were subjected to RNA-seq. Comparing the KC transcriptome of the two groups of mice revealed that a total of 1,961 genes were significantly differentially expressed by at least two-fold, of which 797 were upregulated and 1,164 were downregulated in the *Lama3*e KO/B⁺ KCs. The top 10 of the downregulated and upregulated genes in the RNA-seq data-set are shown in Supplementary Figure S2.

To explore in unbiased detail the biological distribution of the large set of upregulated genes and to discover the molecular consequences of *Lama3* inactivation in the epidermis, we applied DAVID bioinformatics tools to analyze the RNA-seq dataset (Huang et al., 2009). Gene ontology enrichment analysis indicated that the most significantly upregulated biological processes in the *Lama3*e KO/B+ mice were associated with KC differentiation, epidermal cell differentiation, skin development, and epithelial cell differentiation (Figure 2a). Indeed, among the different transcripts
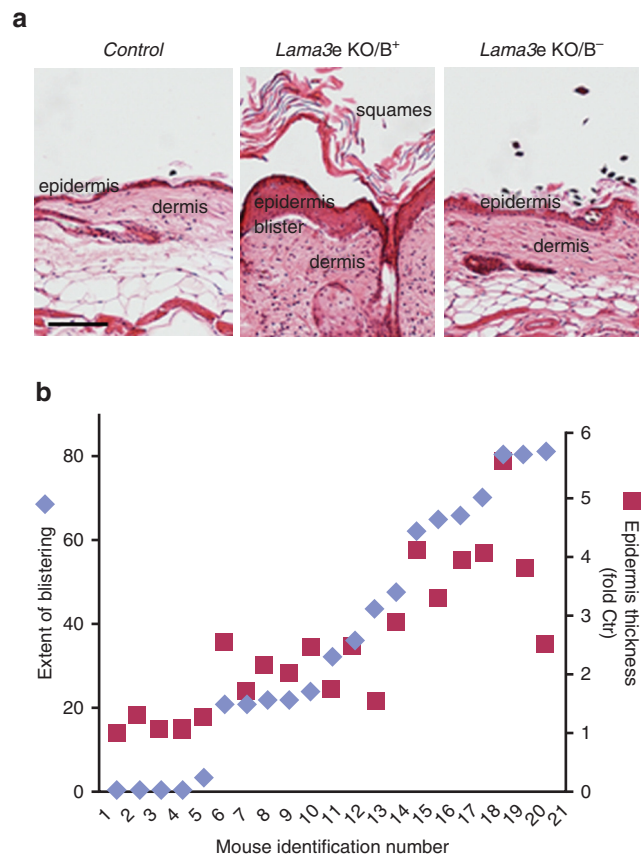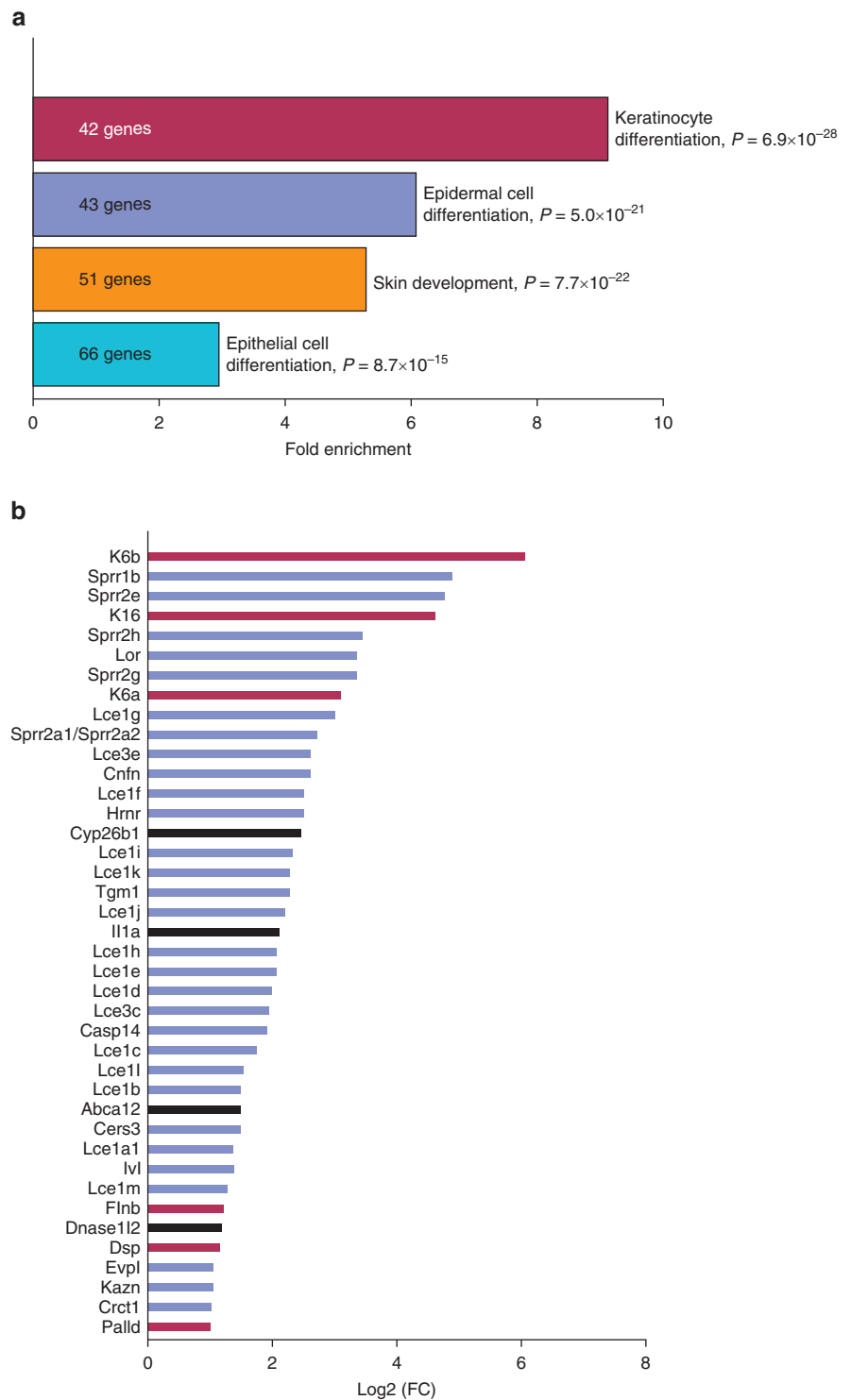

Figure 1. Epidermis thickening above blisters of tamoxifen-treated *Lama3*e KO mice. (**a**) H&E-stained sections of paraffin-embedded back skin from *Lama3*e KO and Ctrl mice after 11 weeks of tamoxifen treatment. The epidermis of *Lama3*e KO mouse with extended blistering (*Lama3*e KO/B⁺) is much thicker than that of the above-nonblistered area (*Lama3*e KO/B⁻) or Ctrl mouse. Bar = 100 μm. (**b**) Length of blistering (blue diamonds; % of the total length of skin section) and epidermal thickness (red squares; fold increase compared with that of the Ctrl) were quantified on H&E-stained skin as in (**a**) for 21 *Lama3*e KO mice and littermate Ctrl. The blue and red symbols of each mouse are aligned vertically. The values for the 21 mice are distributed horizontally and ordered according to the extent of the blistered area, from the lowest value (left; mice 1–10) up to the largest value (right; mice 11–21). Ctrl, control; *Lama3*e KO, *Lama3*e knockout; *Lama3*e KO/B⁺, *Lama3*e knockout mouse with blister; *Lama3*e KO/B⁻, *Lama3*e knockout mouse without blister.

comprising each category, 40 were the same, and the majority of them encode cornified envelope proteins that are a hallmark of KC differentiation (Kypriotou et al., 2012; Oh and de Guzman Strong, 2017). These include genes belonging to the family of SPRRs, involucrin, LCE proteins, and loricrin (Figure 2b, red bars). Expression of genes coding for the cornified envelope components hornerin, cornifelin, and envoplakin—crucial for barrier formation—and genes coding for markers of KC differentiation, such as transglutaminase 1 or caspase 14, were also increased (Figure 2b). In contrast, only two genes (*Crnn* and *Sprr4*) encoding cornified envelope proteins were downregulated (Log₂[fold change] = −4.17 and −2,07, respectively).

Another highly upregulated gene in the top 10 of the RNA-seq dataset is the *Flg* gene encoding FLG (Supplementary Figure S2), the major constituent of the epidermal outermost layer that is crucial for barrier

formation and function (Sandilands et al., 2009). Immunofluorescence staining of the skin of *Lama3*e KO/B$^+$ mice confirmed the upregulation of FLG expression at the protein level, with a massive accumulation of the protein in the stratum corneum (Figure 3a) and an increase in the number of FLG-positive cells within the granular layer of the epidermis (Figure 3b). FLG is a marker of terminally differentiated epidermal cells. Because the granular layer cells commit to terminal differentiation, they form the flattened squames of the stratum corneum (Sandilands et al., 2009). Thus, the upregulation of FLG at both the RNA and protein levels is consistent with the increased presence of squames seen in the H&E-stained epidermis of *Lama3*e KO mice (Figures 1a and 3c).

Taken together, these results show that detachment of basal KCs due to loss of Lm332 in the basement membrane strongly impacts KC differentiation with an exaggerated expression of genes coding for proteins linked to KC
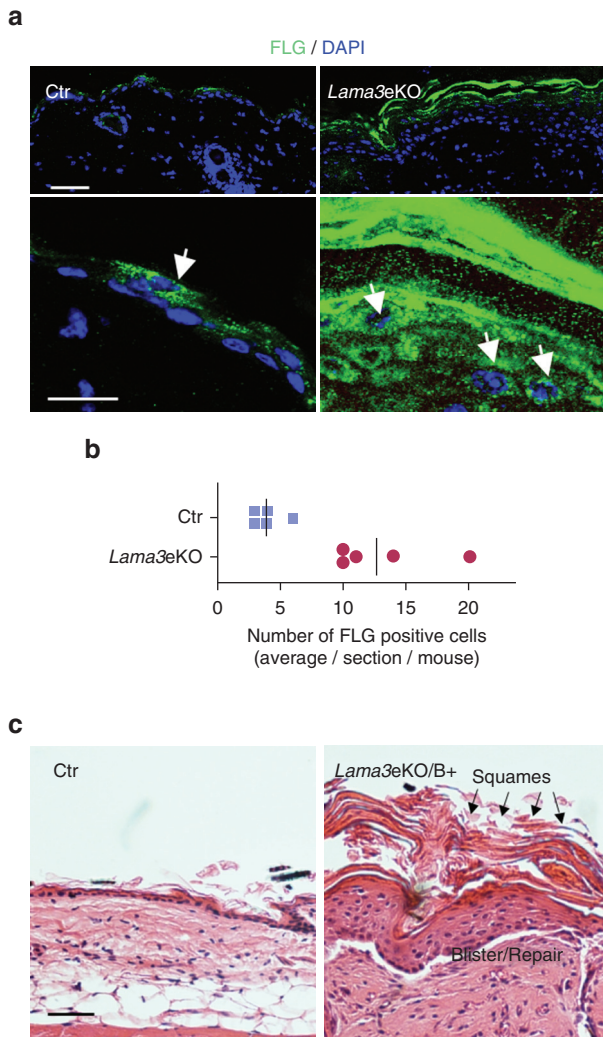
a

FLG / DAPI

b

Number of FLG positive cells
(average / section / mouse)

c

Figure 3. Accumulation of squames and increase of FLG in the uppermost layers of the epidermis of *Lama3*e KO/B$^+$ mice. (**a**) Sections of paraffin-embedded *Lama3*e KO/B$^+$ and Ctr mice skin were stained for FLG (green). Nuclei were visualized with DAPI (blue). Representative images show the thickening of the FLG-positive layers and an increase in the number of FLG-producing cells in the epidermis of Lm332-depleted skin compared with that in the control. Bars = 50 μm (upper panel) and 20 μm (upper panel). (**b**) For quantification, FLG-positive cells (arrows in **a**) were counted on 8−10 fields (×63) per section for five mice for each genotype. Values shown are means per mouse. The red dots denote *Lama3*e KO/B$^+$ mice, and the blue squares denote the controls. (**c**) H&E staining of back skin of *Lama3*e KO/B$^+$ and Ctr mice. Note the accumulation of thick squames at the surface of the thickened epidermis above a large blister in a *Lama3*e KO/B$^+$ mouse. Bar = 50 μm. Ctr, control; *Lama3*e KO, *Lama3*e knockout; *Lama3*e KO/B$^+$, *Lama3*e knockout mouse with blister.

terminal differentiation and proteins important for epidermal barrier formation.

Modification of epidermal keratin expression during the loss of Lm332

Within the top 10 of the downregulated and upregulated genes were several genes coding for keratins (Supplementary Figure S2). In particular, the type-II epithelial keratin (K) 6 isoform b (*K6b*) was the most upregulated gene in the epidermis of *Lama3*e KO/B$^+$ mice (66-fold) (Figures 2b and 4a). This epithelial keratin was expressed at a low level in

control IFE and was highly upregulated on IFE injury, such as during wound repair and in chronic hyperproliferative diseases (Komine et al., 2000; Rothnagel et al., 1999; Wang et al., 2018). Upregulation of the *K6* genes was confirmed by quantitative real-time reverse transcriptase−PCR (QRT-PCR) with RNA isolated from the epidermis of additional *Lama3*e KO/B$^+$ mice presenting with blisters but not from *Lama3*e KO without blister mice with no or very few blisters (Figure 4b). Genes encoding for K6a (*K6a*) and its type-I partner *K16* were also upregulated 8- and 24-fold, respectively, as well as four other keratin genes; two of which are normally expressed in either simple epithelia (*K7*) or non-keratinizing stratifying epithelia (*K78*), whereas *K80* and *K75* are found in hair follicles (Figure 4a). In contrast, 13 keratin genes, many of which are hair follicles specific (*K32*, *K73*, *K26*, *K35*), were strongly downregulated, some for >100-fold compared with those of the controls (Figure 4a). However, because we did not observe an obvious fur-associated phenotype at the time point when tissue was collected, these genes were not investigated further.

Interestingly, *Lama3*e KO mice did not show alterations in the expression of *K14* and *K10* genes, encoding K14 and K10, typically expressed by basal and suprabasal KCs, respectively. To address whether the epidermal thickening was due to an altered balance between the proliferative compartment, characterized by K14 expression, and the differentiated compartment, characterized by K10, immunohistochemistry was performed using these two markers. This analysis revealed a strong expression of K14 also in the suprabasal layers of the expanded epidermis of *Lama3*e KOB+ mice, indicative of an expansion of the proliferative compartment (Figure 4c). In agreement, strong K10 staining was only observed in the upper layers of the thickened epidermis of these mice, which also was expanded in terms of the number of layers, compared with that of the control. To check whether this expansion was accompanied by increased cell proliferation, we performed immunofluorescence detection of the Ki67 proliferation marker. There was no significant difference in the number of proliferating cells present in the epidermis of *Lama3*e KO and control mice, but some Ki67-positive cells were abnormally located in the suprabasal epidermal layers (Supplementary Figure S3). It indicates that the blisters induced during the loss of Lm332 alter the balance in epidermal proliferation and differentiation, resulting in epidermal hyperthickening and hyperkeratinization.

Together, this shows that the loss of Lm332 in the basement membrane underlying basal KCs and the resulting blisters profoundly affect keratin expression and epidermal differentiation.

Upregulation of alarmins on loss of Lm332 and blistering

Further examination of the RNA-seq dataset revealed substantial upregulation of two genes coding for the calcium ion−binding, EF hand-containing proteins *S100A8* and *S100A9*, showing a 45- and 55-fold increase, respectively, in *Lama3*e KO/B$^+$ mice compared with that in the control mice. Upregulation of these genes was further confirmed by QRT-PCR analysis on RNA isolated from epidermal KCs of additional *Lama3*e KO/B$^+$ mice (Figure 5a), indicative of strong
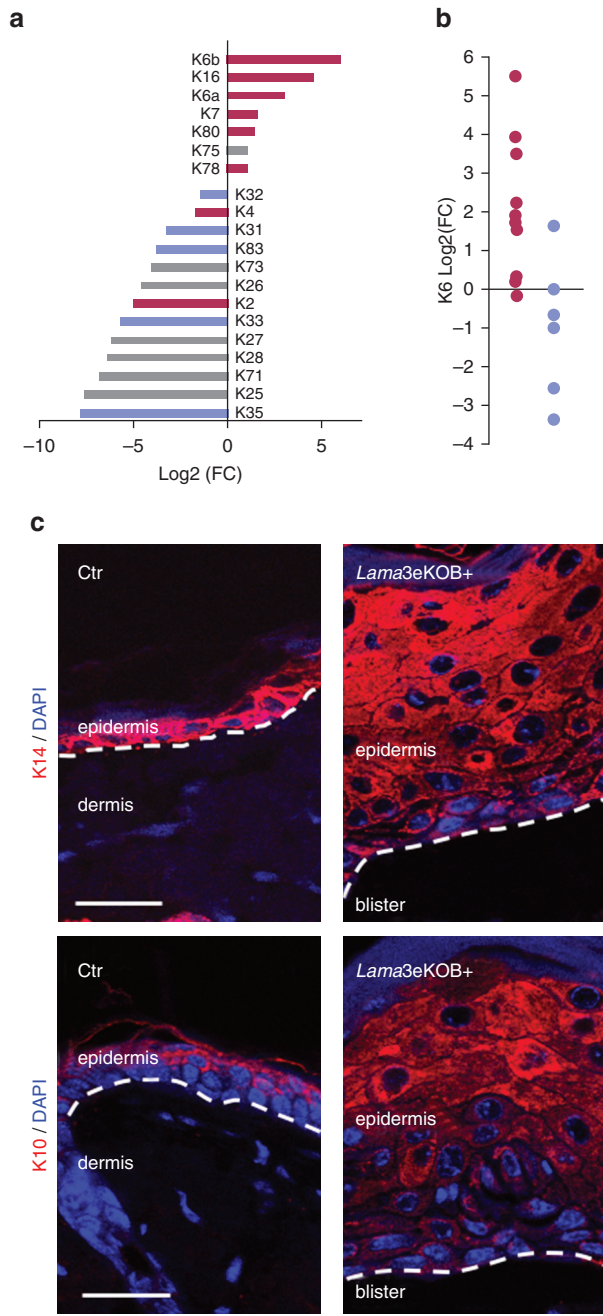
Figure 4. Loss of Lm332 induces a modification in the expression of several keratins in the epidermis of *Lama3e* KO/B$^+$ mice. (**a**) The chart shows Log$_2$(FC) in the RNA-seq dataset (x-axis) for upregulated and downregulated epithelial (red), hair (blue), and hair follicle–specific (gray) K genes indicated along the y-axis. (**b**) Upregulation of K6 was confirmed by QRT-PCR. The results for each *Lama3e* KO mouse were calculated relative to that of the littermate Ctr. The graph shows the results obtained for 16 *Lama3e* KO/B$^+$ mice having developed blisters (red) and 7 *Lama3e* KO/B$^-$ mice with no detected blisters (blue) at the time they were killed. (**c**) Immunofluorescence staining of K10 and K14 on sections of paraffin-embedded back skin of *Lama3e* KO and Ctr mice. K14 is ectopically expressed in the upper layers of the hyperplastic epidermis. Bars = 25 μm. Ctr, control; FC, fold change; K, keratin; *Lama3e* KO, *Lama3e* knockout; *Lama3e* KO/B$^+$, *Lama3e* knockout mouse with blister; *Lama3e* KO/B$^-$, *Lama3e* knockout mouse without blister; Lm332, laminin 332; QRT-PCR, quantitative real-time reverse transcriptase–PCR; RNA-seq, RNA sequencing.
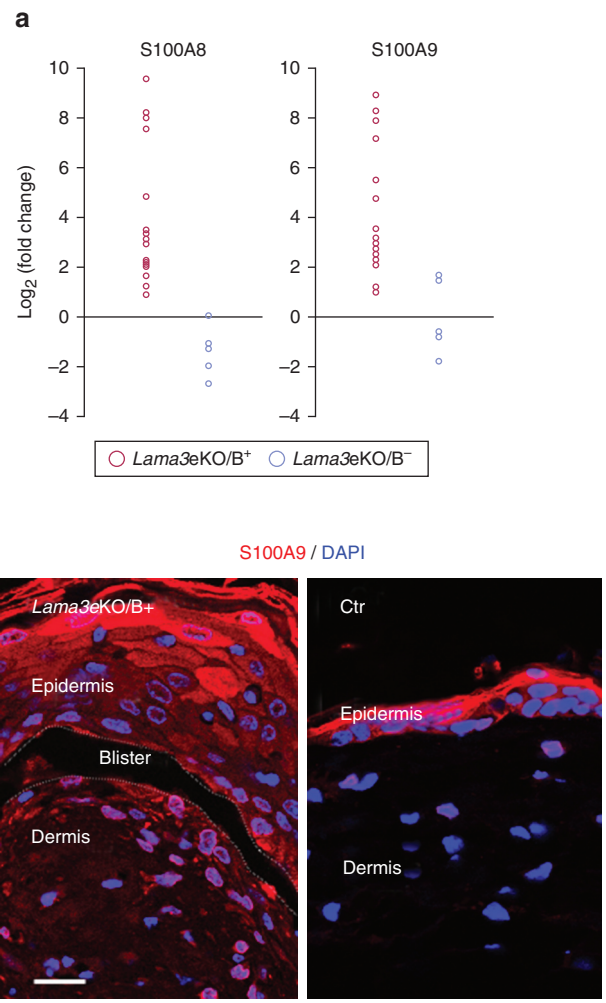

Figure 5. Upregulation of S100A8 and S100A9 alarmins. (**a**) QRT-PCR analysis of S100A8 and S100A9. Each data point represents the results of single *Lama3e* KO mice compared with those of its matched littermate Ctr. The red dots correspond to mice with blisters (*Lama3e* KO/B$^+$), and the blue dots correspond to mice without blisters (*Lama3e* KO/B$^-$) used for comparison. (**b**) Immunofluorescence staining of S100A8 on the skin sections of Ctr and *Lama3e* KO/B$^+$ mice. Several S100A8-strongly-positive keratinocytes are located in the upper layers of the thickened epidermis of *Lama3e* KO/B$^+$ mice. Bar = 25 μm. Ctr, control; *Lama3e* KO, *Lama3e* knockout; *Lama3e* KO/B$^+$, *Lama3e* knockout mouse with blister; *Lama3e* KO/B$^-$, *Lama3e* knockout mouse without blister; QRT-PCR, quantitative real-time reverse transcriptase–PCR.

and sustained KC activation. Interestingly, the upregulation was only observed in the epidermis of *Lama3e* KO/B$^+$ mice with extensive blisters but not in *Lama3e* KO mice with few or no blisters at the time they were killed (Figure 5a). S100A8 and S100A9 proteins represent a subset of alarmins or danger-associated molecular patterns associated with barrier dysfunction, which are essential to initiate and sustain inflammatory responses (Podgórska et al., 2018). These proteins are present at a low level in the normal epidermis, whereas their expression is highly upregulated in abnormally differentiating KCs (Broome et al., 2003; Thorey et al., 2001; Zenz et al., 2005). In agreement, immunofluorescence staining of S100A9 in the thickened epithelium above the blisters

developed in Lm332-depleted skin showed strongly positive cells in the upper epidermal layers of *Lama3*e KO/B$^+$ mice (Figure 5b). These data support the abnormalities characterized earlier in epidermal homeostasis on depletion of Lm332 and point to the presence of inflammation in the blister-containing regions of the IFE.

Loss of adhesion to Lm332 induces a distinct change in the shape of basal KCs

The keratin network is a major determinant of KC shape and intercellular junctions (Simpson et al., 2011). Because the expression of keratins is strongly affected in the epidermis of *Lama3*e KO mice (Figure 4), we wondered whether this had an effect on the morphology of KCs and their intercellular junctions. To answer the question, the KCs were stained for β-catenin to mark junctions and overall cell shape. Analysis of β-catenin–staining pattern showed that intercellular junctions were clearly decorated in the epidermis of both *Lama3*e KO and control mice but that the shape of epidermal cells differed (Figure 6a). In the epidermis of control mice, the roughly cuboid basal KCs were well-aligned along the dermal–epidermal junction, and the suprabasal KCs were typically flattened. In contrast, basal and suprabasal KCs could not be distinguished by their morphology in the detached epidermis of *Lama3*e KO mice (Figure 6a).

Cell shape is dependent on the actomyosin cytoskeleton adapting to a balance between internal and external forces (Pollard and Cooper, 2009). To check the integrity of the cytoskeleton, filamentous actin was visualized by fluorescent phalloidin (Figure 6b). In the control skin, the contours of basal KCs were well-delineated by a circumferential staining of filamentous actin. In contrast, for *Lama3*e KO/B$^+$ mice, the filamentous-actin cytoskeletal network was disorganized either partially in the epidermal cells present in areas where a blister has not yet developed or totally in epidermal cells located in the roof of the blisters.

Finally, the *Acta2* gene coding for α-smooth muscle actin isoform was found elevated in the RNA-seq dataset (Log$_2$[fold change] = 3.54125). QRT-PCR analysis confirmed the expression of *Acta2* RNA isolated from epidermal KCs of additional *Lama3*e KO/B$^+$ mice (Figure 6c). Immunofluorescence staining showed aberrant expression of α-smooth muscle actin in epidermal cells lining the roof of the blisters developed in *Lama3*e KO/B$^+$ mice, whereas the protein was typically absent in the basal KCs of the control mice (Figure 6d). Taken together, the results show that the overall cell–cell and cell–matrix adhesion machinery is affected during the loss of epidermal Lm332.

DISCUSSION

In this work, we show that inactivation of the *Lama3* gene in adult mouse skin, causing loss of Lm332 and blistering along the IFE, provokes the thickening of the epidermis and alters the KC differentiation program.

The essential role of Lm332 for anchoring of the epidermis to the dermis has been firmly established by the genetics of epidermolysis bullosa in humans or the constitutive deletion of coding genes in mice (Kuster et al., 1997; Meng et al.,
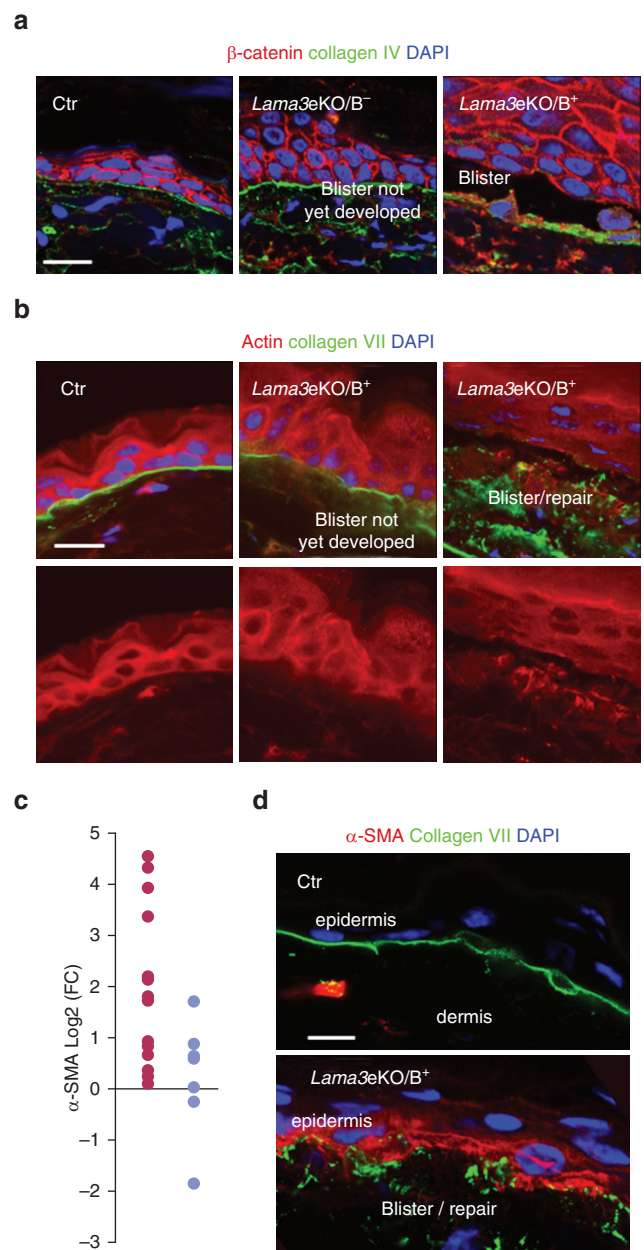

Figure 6. Staining of intercellular junctions and actin isoforms in the epidermis of *Lama3*e KO/B$^+$ mice. (**a**) Paraffin-embedded sections of Ctr mice and mice with (*Lama3*e KO/B$^+$) and without (*Lama3*e KO/B$^-$) blisters were stained for β-catenin (red) and collagen IV (green). Bar = 15 μm. (**b**) Cryosections were stained for fibrillar actin (red) and collagen VII (green) in the Ctr and *Lama3*e KO/B$^+$ mice. Pictures show the areas with and without blisters as indicated. Actin staining is superimposed with other stainings (upper row) or shown as single color (lower row). The circumferential actin network in Ctr epidermis has disappeared in *Lama3*e KO/B$^+$ mice. Bar = 15 μm. (**c**) QRT-PCR analysis of α-smooth muscle actin. Log$_2$(FC) (x-axis) is shown for individual *Lama3*e KO/B$^+$ (red) and *Lama3*e KO/B$^-$ (blue) mouse compared with that of the littermate Ctr. (**d**) Immunofluorescence staining of α-SMA (red) and collagen VII (green) in Ctr and *Lama3*e KO mice. Bar = 5 μm. α-SMA, α-smooth muscle actin; Ctr, control; FC, fold change; *Lama3*e KO, *Lama3*e knockout; *Lama3*e KO/B$^+$, *Lama3*e knockout mouse with blister; *Lama3*e KO/B$^-$, *Lama3*e knockout mouse without blister; QRT-PCR, quantitative real-time reverse transcriptase−PCR.

2003; Ryan et al., 1999; Uitto et al., 1994). At the molecular level, this is mediated by a direct interaction between Lm332 and α6β4 integrins expressed by basal KCs (Niessen et al., 1994; Rousselle and Aumailley, 1994). In contrast, few in vivo studies support a role of Lm332 in other cellular activities such as migration, differentiation, survival, growth, or gene expression described in vitro and mediated by the interaction of Lm332 with cellular receptors, mainly the α3β1 and α6β4 integrins (Carter et al., 1990; Mainiero et al., 1997; Russell et al., 2003; Niessen et al., 1994; Wang et al., 2020; Zhang et al., 2011). A slightly impaired KC survival is observed in newborn mice with disruption of genes encoding Lm332 or its α3β1 and α6β4 receptors (DiPersio et al., 2000; Dowling et al., 1996; Georges-Labouesse et al., 1996; Kuster et al., 1997; Meng et al., 2003; Raymond et al., 2005; Ryan et al., 1999; van der Neut et al., 1996). A small increase in FLG and involucrin was observed in mouse embryonic KCs with deletion of the α6 integrin (Rodius et al., 2007), and a moderate increase in envoplakin and desmoglein 1 mRNAs was reported for newborn mice after inactivation of the *Lamc2* gene (Meng et al., 2003). Thus, Lm332 and its signaling through integrins are dispensable for skin morphogenesis before birth, in accordance with the fact that the epidermis develops and differentiates without Lm332 being expressed up to E15 in the mouse (Aberdam et al., 1994) and 6−8 weeks gestation in humans (Lu et al., 2001; Miosge et al., 2002).

In contrast, our results show that Lm332 is not only essential for epidermis anchorage in adult skin but also for epidermal homeostasis. Its loss leads to epidermal thickening, including alterations in KC terminal differentiation and stratification.

The C-terminus of Lm332 interacts with hemidesmosomal integrins, whereas its N-terminus binds collagen VII, which in turn entraps interstitial collagen fibers in the upper dermis (Krieg and Aumailley, 2011). Interestingly, there is no compensatory mechanism for the loss of Lm332-mediated cell anchorage. Although other laminins with the same integrin-binding repertoire as Lm332 are present underneath basal KCs (Aumailley and Rousselle, 1999; McMillan et al., 2006; Morgner et al., 2015), none has the property of binding to collagen VII, which may explain the lack of compensation. Thus, Lm332 seems to be irreplaceable in the multiprotein complex connecting the keratin network to the collagen network of the upper dermis.

Epidermal homeostasis results from a balance between cell proliferation in the basal layer and terminal cell differentiation in the upper layers of the epidermis, ultimately leading to desquamation. This balance seems broken in the epidermis of *Lama3*e KO mice, especially over the blisters. We did not find an indication of excessive proliferation of KCs, although the process of terminal differentiation was strongly induced. This is reminiscent of the terminal differentiation elicited when human epidermal KCs are shifted from monolayer to suspension cultures (Rice and Green, 1978). We previously observed the thickening of the epidermis with a normal number of proliferating basal KCs after deletion of the *Ilk* gene, which weakens integrin-mediated KC adhesion to Lm332 (Lorenz et al., 2007). Epidermal thickening associated with acanthosis and hyperkeratosis but not with a major

increase in cell proliferation is also seen in a mouse model of bullous congenital ichthyosiform erythroderma (Porter et al., 1998). In this model, epidermal thickening was caused by decreased desquamation rather than by an increase in cell proliferation. A similar mechanism could be responsible for epidermis thickening in *Lama3*e KO mice.

A balance between the tensile forces transmitted through the cytoskeleton guarantees the maintenance of cell and tissue homeostasis, including in the skin (Biggs et al., 2020; Du et al., 2018). In the epidermis, keratin filaments attached to hemidesmosomes and desmosomes relay the forces emanating from the extracellular matrix and the forces developed across lateral–apical cell contacts, respectively, whereas the actin cytoskeleton and the associated linker proteins mechanically tether the extracellular environment to the nucleus (Lecuit and Yap, 2015; Miroshnikova et al., 2018; van Bodegraven and Etienne-Manneville, 2020). Consequently, the balance between these different forces regulates cellular and nuclear shape but also impacts transcription and chromatin architecture (Miroshnikova et al., 2019). In our *Lama3 KO* mice, we hypothesize that the rearrangement of the actomyosin and keratin networks induced by the loss of Lm332 and concomitant loss of adhesion of the epidermal cells located in the roof of the blisters could profoundly modify mechanosensitive signaling pathways. Interestingly, recent studies on mouse epidermal KCs identified multiple topologically associating domains within the chromatin locus harboring 61 genes of the epidermal differentiation complex, implying a concerted response of the entire locus to changes in mechanotransduction (Poterlowicz et al., 2017). This scenario is a likely explanation for the induction of many of the genes coding for the epidermal differentiation complex in our mouse model.

Interestingly, it has been reported that mechanical stretch results in epidermal thickening in skin equivalents (Tokuyama et al., 2015) and in skin expansion in vivo (Aragona et al., 2020; Rübsam and Niessen, 2020). In conclusion, the maintenance of homeostasis of the adult epidermis depends on the anchoring of basal KCs through Lm332, thereby preventing cellular stress and ensuring the mechanotransduction of signals emanating from the extracellular matrix in the upper dermis and reaching the nucleus of the basal KCs in the epidermis.

MATERIALS AND METHODS
Additional details are provided in the Supplementary Materials and Methods.

Mice
The *Lama3*flox/flox/K14-CreERT (*Lama3*e KO) and *Lama3*wt/flox/K14-CreERT (control) mice were previously described (Pesch et al., 2017). Mice were kept and bred in compliance with the German regulations for the welfare of laboratory animals. Experiments were licensed by the North Rhine-Westphalia State Environmental Agency, Germany.

Histology, immunocytochemistry, immunofluorescence, SDS-PAGE, immunoblotting
These techniques followed standard procedures as described in the study by Pesch et al. (2017).

Morphometric analysis

On light microscopy photographs of H&E-stained back skin sections (three sections per mouse), the total length of the dermal–epidermal junction seen on the section with (designated as a) and without (designated as b) blisters was measured with ImageJ (https://imageJ.nih.gov). The extent of blistering was expressed as a / a+b. For epidermal thickness, measurements (10 per section) were randomly performed along the section for control mice and in areas above the blisters for *Lama3*e KO mice.

RNA preparation and sequencing and QRT-PCR

Skin flaps from tamoxifen-treated *Lama3* KO and control mice (~1 cm^2) were bathed in 0.8% trypsin in PBS for 60 minutes at 37 °C to allow the detaching of the epidermis from the dermis. Epidermal cells were dispersed by pipetting, collected by centrifugation, and used for preparation, analysis, and sequencing of RNAs (three biological replicates per condition). Transcripts regulated more than two-fold and with an adjusted $P \leq 0.05$ were used for analysis with the DAVID bioinformatics resource (Huang et al., 2009). RNA-seq data have been deposited to National Center for Biotechnology Information-Gene Expression Omnibus (GSE146045). QRT-PCR was performed according to standard procedures.

Data availability statement

RNA sequencing data have been deposited to National Center for Biotechnology Information-Gene Expression Omnibus (GSE146045).

ORCIDs
Raneem Tayem: http://orcid.org/0000-0001-5178-9353
Catherin Niemann: http://orcid.org/0000-0002-7224-6216
Monika Pesch: http://orcid.org/0000-0003-0884-1819
Jessica Morgner: http://orcid.org/0000-0001-6374-8639
Carien M. Niessen: http://orcid.org/0000-0002-4892-9391
Sara A. Wickström: http://orcid.org/0000-0001-6383-6292
Monique Aumailley: http://orcid.org/0000-0002-4578-0966

CONFLICT OF INTEREST
CMN is an unpaid scientific advisor of Mane Biotech. The remaining authors state no conflict of interest

AUTHOR CONTRIBUTIONS
Conceptualization: MA, SAW; Data Curation; MA, SAW, CN, CMN; Methodology: RT, MP, JM, CN; Supervision: MA; Writing - Original Draft Preparation: MA; Writing - Review and Editing: JM, SAW, CN, CMN

SUPPLEMENTARY MATERIAL
Supplementary material is linked to the online version of the paper at www.jidonline.org, and at https://doi.org/10.1016/j.jid.2021.04.008.

REFERENCES

Aberdam D, Aguzzi A, Baudoin C, Galliano MF, Ortonne JP, Meneguzzi G. Developmental expression of nicein adhesion protein (laminin-5) subunits suggests multiple morphogenic roles. Cell Adhes Commun 1994;2: 115−29.

Aragona M, Sifrim A, Malfait M, Song Y, Van Herck J, Dekoninck S, et al. Mechanisms of stretch-mediated skin expansion at single-cell resolution. Nature 2020;584:268−73.

Aumailley M. The laminin family. Cell Adh Migr 2013;7:48−55.

Aumailley M, Has C, Tunggal L, Bruckner-Tuderman L. Molecular basis of inherited skin-blistering disorders, and therapeutic implications. Expert Rev Mol Med 2006;8:1−21.

Aumailley M, Rousselle P. Laminins of the dermo-epidermal junction. Matrix Biol 1999;18:19−28.

Biggs LC, Kim CS, Miroshnikova YA, Wickström SA. Mechanical forces in the skin: roles in tissue architecture, stability, and function. J Invest Dermatol 2020;140:284−90.

Broome AM, Ryan D, Eckert RL. S100 protein subcellular localization during epidermal differentiation and psoriasis. J Histochem Cytochem 2003;51: 675−85.

Carter WG, Kaur P, Gil SG, Gahr PJ, Wayner EA. Distinct functions for integrins alpha 3 beta 1 in focal adhesions and alpha 6 beta 4/bullous pemphigoid antigen in a new stable anchoring contact (SAC) of keratinocytes: relation to hemidesmosomes. J Cell Biol 1990;111:3141−54.

DiPersio CM, van der Neut R, Georges-Labouesse E, Kreidberg JA, Sonnenberg A, Hynes RO. Alpha 3 beta 1 and alpha 6 beta 4 integrin receptors for laminin-5 are not essential for epidermal morphogenesis and homeostasis during skin development. J Cell Sci 2000;113:3051−62.

Dowling J, Yu QC, Fuchs E. Beta 4 Integrin is required for hemidesmosome formation, cell adhesion and cell survival. J Cell Biol 1996;134:559−72.

Du H, Wang Y, Haensel D, Lee B, Dai X, Nie Q. Multiscale modeling of layer formation in epidermis. PLoS Comput Biol 2018;14:e1006006.

Durbeej M. Laminin-α2 chain-deficient congenital muscular dystrophy: pathophysiology and development of treatment. Curr Top Membr 2015;76: 31−60.

Funk SD, Lin MH, Miner JH. Alport syndrome and Pierson syndrome: diseases of the glomerular basement membrane. Matrix Biol 2018;71−72:250−61.

Georges-Labouesse E, Messaddeq N, Yehia G, Cadalbert L, Dierich A, Le Meur M. Absence of integrin alpha 6 leads to epidermolysis bullosa and neonatal death in mice. Nat Genet 1996;13:370−3.

Huang da W, Sherman BT, Lempicki RA. Systematic and integrative analysis of large gene lists using DAVID Bioinformatics Resources. Nat Protoc 2009;4:44−57.

Kiritsi D, Has C, Bruckner-Tuderman L. Laminin 332 in junctional epidermolysis bullosa. Cell Adh Migr 2013;7:135−41.

Komine M, Rao LS, Kaneko T, Tomic-Canic M, Tamaki K, Freedberg IM, et al. Inflammatory versus proliferative processes in epidermis. Tumor necrosis factor alpha induces K6b keratin synthesis through a transcriptional complex containing NFkappaB and C/EBPbeta. J Biol Chem 2000;275:32077−88.

Krieg T, Aumailley M. The extracellular matrix of the dermis: flexible structures with dynamic functions. Exp Dermatol 2011;20:689−95.

Kuster JE, Guarnieri MH, Ault JG, Flaherty L, Swiatek PJ. IAP Insertion in the murine lamB3 gene results in junctional epidermolysis bullosa. Mamm Genome 1997;8:673−81.

Kypriotou M, Huber M, Hohl D. The human epidermal differentiation complex: cornified envelope precursors, S100 proteins and the 'fused genes' family. Exp Dermatol 2012;21:643−9.

Lecuit T, Yap AS. E-cadherin junctions as active mechanical integrators in tissue dynamics. Nat Cell Biol 2015;17:533−9.

Lorenz K, Grashoff C, Torka R, Sakai T, Langbein L, Bloch W, et al. Integrin-linked kinase is required for epidermal and hair follicle morphogenesis. J Cell Biol 2007;177:501−13.

Lu W, Miyazaki K, Mizushima H, Nemoto N. Immunohistochemical distribution of laminin-5 γ2 chain and its developmental change in human embryonic and foetal tissues. Histochem J 2001:629−37.

Mainiero F, Murgia C, Wary KK, Curatola AM, Pepe A, Blumemberg M, et al. The coupling of α6β4 integrin to Ras-MAP kinase pathways mediated by Shc controls keratinocyte proliferation. EMBO J 1997;16:2365−75.

McMillan JR, Akiyama M, Nakamura H, Shimizu H. Colocalization of multiple laminin isoforms predominantly beneath hemidesmosomes in the upper lamina densa of the epidermal basement membrane. J Histochem Cytochem 2006;54:109−18.

Meng X, Klement JF, Leperi DA, Birk DE, Sasaki T, Timpl R, et al. Targeted inactivation of murine laminin γ2-chain gene recapitulates human junctional epidermolysis bullosa. J Invest Dermatol 2003;121:720−31.

Miosge N, Kluge JG, Studzinski A, Zelent C, Bode C, Sprysch P, et al. In situ-RT-PCR and immunohistochemistry for the localisation of the mRNA of the

α3 chain of laminin and laminin-5 during human organogenesis. Anat Embryol (Berl) 2002;205:355—63.

Miroshnikova YA, Cohen I, Ezhkova E, Wickström SA. Epigenetic gene regulation, chromatin structure, and force-induced chromatin remodelling in epidermal development and homeostasis. Curr Opin Genet Dev 2019;55:46—51.

Miroshnikova YA, Le HQ, Schneider D, Thalheim T, Rübsam M, Bremicker N, et al. Adhesion forces and cortical tension couple cell proliferation and differentiation to drive epidermal stratification. Nat Cell Biol 2018;20: 69—80.

Morgner J, Ghatak S, Jakobi T, Dieterich C, Aumailley M, Wickström SA. Integrin-linked kinase regulates the niche of quiescent epidermal stem cells. Nat Commun 2015;6:8198.

Niessen CM, Hogervorst F, Jaspars LH, de Melker AA, Delwel GO, Hulsman EH, et al. The alpha 6 beta 4 integrin is a receptor for both laminin and kalinin. Exp Cell Res 1994;211:360—7.

Oh IY, de Guzman Strong C. The molecular revolution in cutaneous biology: EDC and locus control. J Invest Dermatol 2017;137:e101—4.

Pesch M, König S, Aumailley M. Targeted disruption of the Lama3 gene in adult mice is sufficient to induce skin inflammation and fibrosis. J Invest Dermatol 2017;137:332—40.

Podgórska M, Ołdak M, Marthaler A, Fingerle A, Walch-Rückheim B, Lohse S, et al. Chronic inflammatory microenvironment in epidermodysplasia verruciformis skin lesions: role of the synergism between HPV8 E2 and C/EBPβ to induce pro-inflammatory S100A8/A9 proteins. Front Microbiol 2018;9: 392.

Pollard TD, Cooper JA. Actin, a central player in cell shape and movement. Science 2009;326:1208—12.

Porter RM, Reichelt J, Lunny DP, Magin TM, Lane EB. The relationship between hyperproliferation and epidermal thickening in a mouse model for BCIE. J Invest Dermatol 1998;110:951—7.

Poterlowicz K, Yarker JL, Malashchuk I, Lajoie BR, Mardaryev AN, Gdula MR, et al. 5C analysis of the Epidermal Differentiation Complex locus reveals distinct chromatin interaction networks between gene-rich and gene-poor TADs in skin epithelial cells. PLoS Genet 2017;13:e1006966.

Qin Y, Rodin S, Simonson OE, Hollande F. Laminins and cancer stem cells: partners in crime? Semin Cancer Biol 2017;45:3—12.

Raymond K, Kreft M, Janssen H, Calafat J, Sonnenberg A. Keratinocytes display normal proliferation, survival and differentiation in conditional beta 4-integrin knockout mice. J Cell Sci 2005;118:1045—60.

Rice RH, Green H. Relation of protein synthesis and transglutaminase activity to formation of the cross-linked envelope during terminal differentiation of the cultured human epidermal keratinocyte. J Cell Biol 1978;76:705—11.

Rodius S, Indra G, Thibault C, Pfister V, Georges-Labouesse E. Loss of alpha 6 integrins in keratinocytes leads to an increase in TGFbeta and AP1 signaling and in expression of differentiation genes. J Cell Physiol 2007;212:439—49.

Rothnagel JA, Seki T, Ogo M, Longley MA, Wojcik SM, Bundman DS, et al. The mouse keratin 6 isoforms are differentially expressed in the hair follicle, footpad, tongue and activated epidermis. Differentiation 1999;65: 119—30.

Rousselle P, Aumailley M. Kalinin is more efficient than laminin in promoting adhesion of primary keratinocytes and some other epithelial cells

and has a different requirement for integrin receptors. J Cell Biol 1994;125:205—14.

Rübsam M, Niessen CM. Stretch exercises for stem cells expand the skin. Nature 2020;584:196—8.

Russell AJ, Fincher EF, Millman L, Smith R, Vela V, Waterman EA, et al. Alpha 6 beta 4 Integrin regulates keratinocyte chemotaxis through differential GTPase activation and antagonism of alpha 3 beta 1 integrin. J Cell Sci 2003;116:3543—56.

Ryan MC, Lee K, Miyashita Y, Carter WG. Targeted disruption of the LAMA3 gene in mice reveals abnormalities in survival and late stage differentiation of epithelial cells. J Cell Biol 1999;145:1309—23.

Sandilands A, Sutherland C, Irvine AD, McLean WH. Filaggrin in the frontline: role in skin barrier function and disease. J Cell Sci 2009;122:1285—94.

Simon T, Bromberg JS. Regulation of the immune system by laminins. Trends Immunol 2017;38:858—71.

Simpson CL, Patel DM, Green KJ. Deconstructing the skin: cytoarchitectural determinants of epidermal morphogenesis. Nat Rev Mol Cell Biol 2011;12: 565—80.

Thorey IS, Roth J, Regenbogen J, Halle JP, Bittner M, Vogl T, et al. The Ca2+-binding proteins S100A8 and S100A9 are encoded by novel injury-regulated genes. J Biol Chem 2001;276:35818—25.

Tokuyama E, Nagai Y, Takahashi K, Kimata Y, Naruse K. Mechanical stretch on human skin equivalents increases the epidermal thickness and develops the basement membrane. PLoS One 2015;10:e0141989.

Uitto J, Pulkkinen L, Christiano AM. Molecular basis of the dystrophic and junctional forms of epidermolysis bullosa: mutations in the type VII collagen and kalinin (laminin 5) genes. J Invest Dermatol 1994;103(Suppl. 5):39S—46S.

van Bodegraven EJ, Etienne-Manneville S. Intermediate filaments against actomyosin: the david and goliath of cell migration. Curr Opin Cell Biol 2020;66:79—88.

van der Neut R, Krimpenfort P, Calafat J, Niessen CM, Sonnenberg A. Epithelial detachment due to absence of hemidesmosomes in integrin beta 4 null mice. Nat Genet 1996;13:366—9.

Wang F, Chen S, Liu HB, Parent CA, Coulombe PA. Keratin 6 regulates collective keratinocyte migration by altering cell-cell and cell-matrix adhesion. J Cell Biol 2018;217:4314—30.

Wang W, Zuidema A, Te Molder L, Nahidiazar L, Hoekman L, Schmidt T, et al. Hemidesmosomes modulate force generation via focal adhesions. J Cell Biol 2020;219:e201904137.

Zenz R, Eferl R, Kenner L, Florin L, Hummerich L, Mehic D, et al. Psoriasis-like skin disease and arthritis caused by inducible epidermal deletion of Jun proteins [published correction appears in Nature 2006;440:708]. Nature 2005;437:369—75.

Zhang Z, Chometon G, Wen T, Qu H, Mauch C, Krieg T, et al. Migration of epithelial cells on laminins: RhoA antagonizes directionally persistent migration. Eur J Cell Biol 2011;90:1—12.

SUPPLEMENTARY MATERIALS AND METHODS

Mice

An epidermis-specific, inducible deletion of the *Lama3* gene (coding for the laminin α3 chain) was obtained by crossing mice with a floxed *Lama3* gene (*Lama3*flox/flox) with keratin (K) 14-driven Cre deleter mice expressing the Cre recombinase fused to a mutated ligand-binding domain of the human estrogen receptor (K14-CreERT). Offsprings were phenotypically indistinguishable. Ear DNA was used for genotyping by PCR with the following primers: 5′-GCGGTCTGGCAG-TAAAAACTATC-3′ (forward) and 5′-GTGAAA-CAGCATTGCTGTCACTT-3′ (reverse) for the K14-CreERT transgene and 5′-GGCAGGGACTTTCTTTCTGG-3′ (forward) and 5′-GCATCAGATCTCATTACAGATGG-3′ (reverse) for the wild-type and floxed alleles. For these studies, the following genotypes were used for experiments: *Lama3*flox/flox/K14-CreERT and *Lama3*wt/flox/K14-CreERT. Feeding the mice with a tamoxifen-containing chow (400 mg tamoxifen citrate per 1 kg of chow; Harlan Netherlands B.V., Venray, The Netherlands) resulted in the activation of the Cre recombinase in the K14-expressing basal cells and consequently in the inactivation of the *Lama3* gene followed by a progressive loss of Lm332 in the *Lama3*flox/flox/K14-CreERT mice but not in the *Lama3*wt/flox/K14-CreERT mice used as controls (Pesch et al., 2017).

Histology

Mice were killed, shaved, and examined for gross alterations of the skin surface. Biopsies taken from the back skin were processed for immediate embedding in Tissue Tek (Sakura Finetek, Staufen, Germany) or for fixation in 4% paraformaldehyde overnight and in paraffin embedding. Sections of 7 μm and 16 μm were made from paraffin-embedded or frozen skin, respectively. H&E staining was done according to standard procedures.

Immunocytochemistry and immunofluorescence

For immunofluorescence staining, slices of paraffin-embedded skin were deparaffinized. Antigens were retrieved either by trypsin treatment or by heat-induced antigen retrieval using citrate (10 mM, pH 6.0) or Tris-Base (10 mM, pH 9, 1mM EDTA, Sigma-Aldrich, St. Louis, MO) buffers in a pressure cooker for 20 minutes. After washing with PBS and blocking in 10% normal goat serum at room temperature, primary antibodies were applied overnight at 4 °C in a humidified chamber. For cryosections, primary antibodies were applied for 90 minutes at room temperature. The following antibodies were used: Cy3-conjugated mouse monoclonal against α-smooth muscle actin (clone 1A4, Sigma-Aldrich); rabbit (Covance, Princeton, NJ) or guinea pig (Progen, Heidelberg, Germany) antiserum against K14; rabbit antisera against K10 (BioLegend, San Diego, CA), FLG (Covance), collagen VII (kindly donated by Dr Sakai, Portland, OR), S100A9 (Life Technologies, Carlsbad, CA), collagen XVII (Abcam, Berlin, Germany), β-catenin (Sigma-Aldrich), and Ki67 (Cell Marque distributed by Medac-diagnostika, Wedel, Germany); and goat antiserum against collagen IV (Temecula, CA); fibrillar actin was stained with coumarin- or TRIC-conjugated phalloidin (Sigma-Aldrich). After washing with PBS, secondary antibodies were applied for 90 minutes in the dark, together with DAPI. Staining was observed with a laser scanning confocal microscope (×10 air, ×40 oil, and ×63 oil objectives (Leica Camera, Wetzlar, Germany). Images were captured with single-channel excitation, stored using the Leica confocal software, and mounted with Photoshop CS6 (Adobe Systems, San Jose, CA).

SDS-PAGE and immunoblotting

To quantify the content in Lm332, pieces of mouse skin frozen in liquid nitrogen were ground with a pestle in a mortar. Proteins were sequentially extracted in Tris-buffered saline containing 20 mM EDTA and 4 M urea, and the protein mixture was fractionated by SDS-PAGE on 7% acrylamide gels under reducing conditions. Samples were loaded onto the gels in duplicate. Immunoblotting was performed as previously described with goat antibody against laminin γ2 chain (sc7652, Santa Cruz Biotechnology, Heidelberg, Germany), rabbit antibody against laminin γ1 chain (sc5584, Santa Cruz Biotechnology), and mouse antibody against actin (clone C4, MilliporeSigma, Burlington, MA) used as primary antibodies followed by species-specific horseradish peroxidase–coupled secondary antibodies (Pesch et al., 2017). Densitometry measurement was performed using ImageJ software (National Institutes of Health, Bethesda, MD).
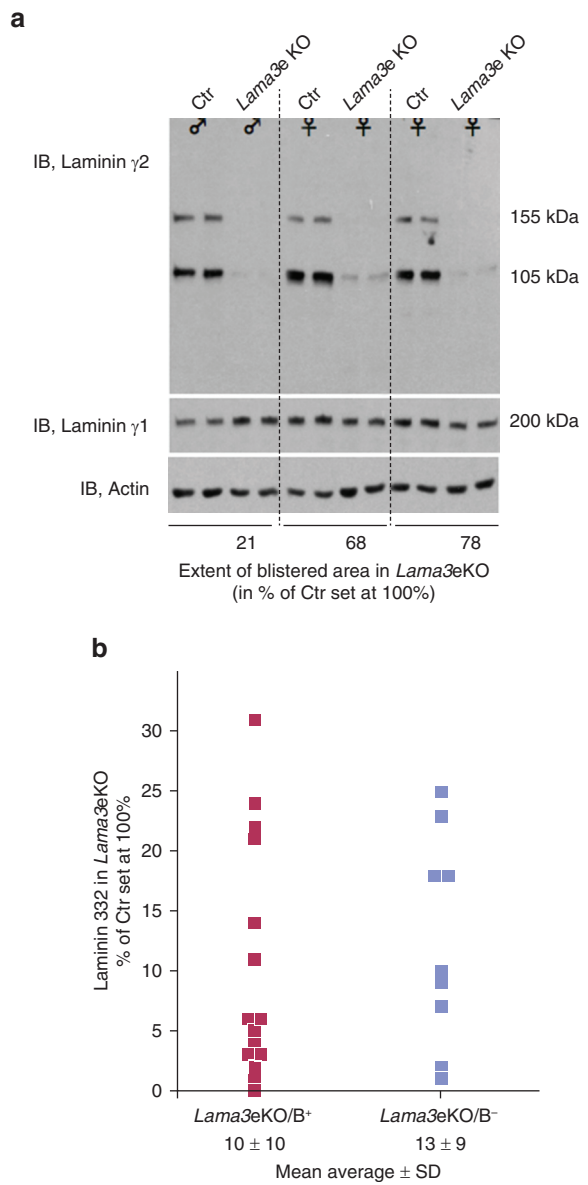
RNA and preparation, RNA sequencing, and quantitative real-time reverse transcriptase–PCR

RNA was prepared with RNeasy Plus Mini Kit (Qiagen, Hilden, Germany) and kept frozen at −80 °C until further use. RNA concentration was determined with the Nanodrop system (Thermo Fisher Scientific, Waltham, MA), and RNA quality control was assessed on Agilent 2100 Bioanalyzer (Agilent Bioanalyzer, Agilent Technologies, Santa Clara, CA). RNAs with an RNA integrity number of at least 8.0 were used for further analysis.

Sequencing was performed with RNAs isolated from tamoxifen-treated Lama3flox/flox / K14-CreERT and control mice (three each). Libraries were prepared with NEBNext Ultra Directional RNA Library Prep Kit (New Englands Biolabs, Ipswich, MA) followed by sequencing with HiSeq 2500 (Illumina, San Diego, CA) from three biological replicates per condition. After quality control and preprocessing, reads were mapped to the *Mus musculus* reference genome (build GRCm38 79), followed by differential gene expression analysis using Cufflinks (version 2.2.1). For quantitative real-time reverse transcriptase–PCR, RNAs were transcribed to cDNA with the High Capacity cDNA Reverse Transcription Kit (Applied Biosystems, Foster City, CA). Quantitative real-time reverse transcriptase–PCR was performed using the SYBR Green Mix in a 7300 Real-Time PCR System (Applied Biosystems, Thermo Fisher Scientific) according to the manufacturer's instructions. The gene-specific primers are listed in Supplementary Table S1. For each mouse, three technical replicates were included in the same run. Relative gene expression was calculated using the $2^{-\Delta\Delta CT}$ method.

SUPPLEMENTARY REFERENCE

Pesch M, König S, Aumailley M. Targeted disruption of the *Lama3* gene in adult mice is sufficient to induce skin inflammation and fibrosis. J Invest Dermatol 2017;137:332−40.

a

IB, Laminin γ2

155 kDa

105 kDa

IB, Laminin γ1 — 200 kDa

IB, Actin

21   68   78

Extent of blistered area in *Lama3*eKO
(in % of Ctr set at 100%)

b

*Lama3*eKO/B⁺   *Lama3*eKO/B⁻
10 ± 10   13 ± 9
Mean average ± SD

Supplementary Figure S1. Content in Lm332 is reduced to a similar extent in the skin of tamoxifen-fed *Lama3*e KO mice with blistering affecting more (*Lama3*e KO/B⁺) or less (*Lama3*e KO/B⁻) than 30% of the interfollicular epidermis. Proteins were extracted from the skin of homozygote *Lama3*e KO and heterozygote *Lama3*^wt/flox^/K14-CreERT (Ctr) mice at the end of the tamoxifen treatment. (**a**) Extracted proteins were fractionated in duplicate by SDS-PAGE under reducing conditions and were immunoblotted with antibodies against laminin γ2, laminin γ1, and actin as indicated. The results obtained for three pairs of *Lama3*e KO mice and respective littermate Ctrs are shown. The amounts of the unprocessed (155 kDa) and processed (105 kDa) laminin γ2 chain are strongly decreased in the skin of *Lama3*e KO mice, whereas the amounts of laminin γ1 chain remain unchanged. Actin was used as the loading control. The extent of skin blistering measured as described in Figure 1 is indicated below the blots for each one of the three *Lama3*e KO mice shown. (**b**) The skin of the 21 *Lama3*e KO mice and littermate controls included in this study was analyzed as described in **a**. Band intensity measurements were used to quantify the total amount (processed plus unprocessed) of laminin γ2 in the skin of *Lama3*e KO and control mice. The scatter plot represents the quantity of laminin γ2 measured for each *Lama3*e KO mouse compared with that of its littermate control set at 100%. The red squares denote the *Lama3*e KO/B⁺ mice with blistering affecting >30% of the length of the dermal–epidermal junction (mice 11–21 in Figure 1); the blue squares denote the *Lama3*e KO/B⁻ mice with blistering affecting <30% of the epidermal–dermal junction (mice 1–10 in Figure 1). The mean average and SD calculated for each group of mice are shown below the plot. Ctr, control; *Lama3*e KO, Lama3e knockout; *Lama3*e KO/B⁺, Lama3e knockout mouse with blister; *Lama3*e KO/B⁻, Lama3e knockout mouse without blister; Lm332, laminin 332.
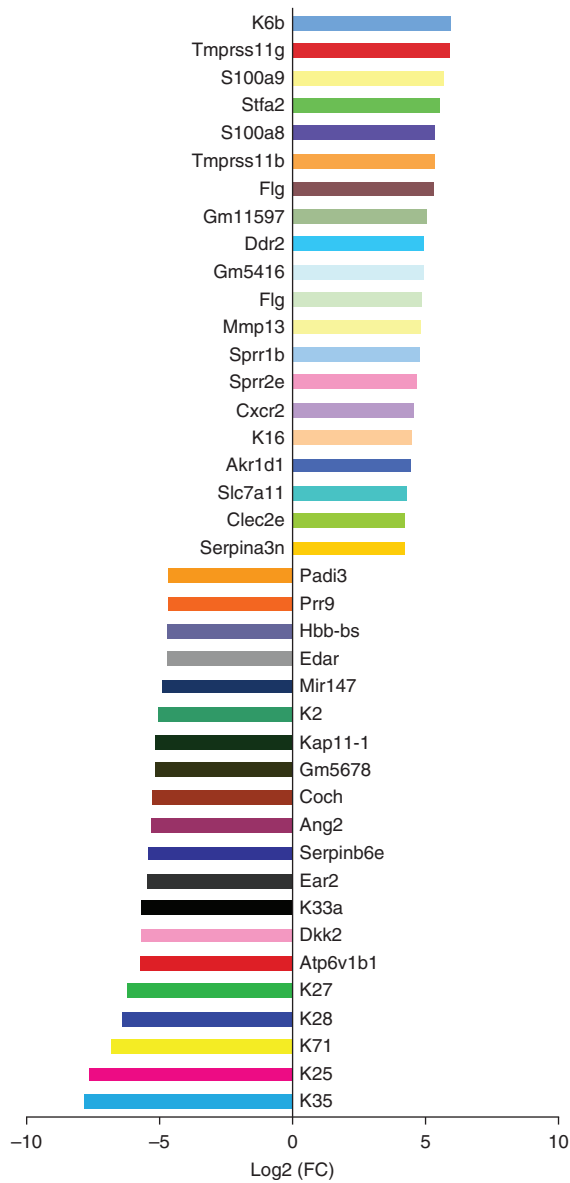
Supplementary Figure S2. The top 20 of the downregulated and upregulated genes in the epidermis of *Lama3*e KO mice. Each bar represents Log$_2$ of FC. The official gene symbols are written on the right (downregulated) and left (upregulated) sides of the bars. FC, fold change; K, keratin; *Lama3* KO, Lama3e knockout.
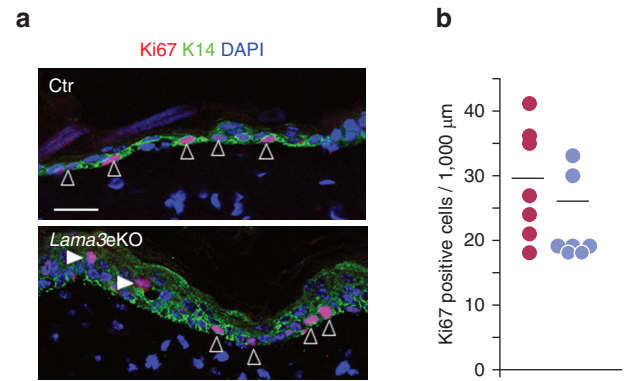
Supplementary Figure S3. Analysis of cell proliferation in the epidermis of *Lama3*e KO/B$^+$ mice. (**a**) Immunofluorescence staining of the cell proliferation markers Ki67 (red) and K14 (green) on paraffin-embedded sections of Ctr and *Lama3*e KO mice. Nuclei were counterstained with DAPI. Proliferating epidermal cells are colored pink (merging red of Ki67 and blue of DAPI). The open arrows indicate the proliferating basal cells, and the white arrows indicate the proliferating epidermal cells with ectopic localization to suprabasal layers. (**b**) The graph shows the number of Ki67-positive cells in the epidermis of *Lama3*e KO (red dots) and Ctr (blue dots) mice. The bar shows the mean average. Ctr, control; K, keratin; *Lama3e* KO, *Lama3*e knockout; *Lama3*e KO/B$^+$, *Lama3*e knockout mouse with blister.

Supplementary Table S1. Primers Used for QRT-PCR

Gene	Forward	Reverse
Actb	tcaagatcattgctcctcctg	tactcctgcttgctgatccac
Acta2	cgagcgtgagattgtccgtg	gtttcgtggatgcccgc
Axin2	agcgccaacgacagcgagtt	aggcggtgggttctcggaaa
K6	ggagagaggggtcgcctggac	ggcagcatctacatccttcttcagg
K14	atcgaggacctgaagagcaa	tcgatctgcaggaggacatt
K35	ctggtatgacacccagaccg	aatgatgtccgactggcagg
K71	agactccgctcagagattg	catccttgagggcactgt
Lama3	cttttctgcaaattggtgggc	catggaagagctgacccagat
Mrps26	ctaccgacagtaccgggaga	atccgtagctcctgcattcg
S100a8	gccgtctgaactggagaag	gtgagatgccacacccacttt
S100a9	cgcagcataaccaccatcat	aagatcaactttgccatcagc

Abbreviations: K, keratin; QRT-PCR, quantitative real-time reverse transcriptase–PCR.